Calibrated simulation of a solar hot water system to match degraded performance over a 22-year period using two models

Larry O. Degelman

Texas A&M University, College Station, TX, USA

Abstract

This paper reports on the measured performance of a residential solar water heating system over a period of 22 years and the modeling of the system to simulate its degradation over that period. The system consists of three fixed flat-plate collectors with a total of $5\,m^2$ of double-layer glass cover plates and black aluminum fin-tube absorber plates. The solar storage tank capacity is 303 L, which is used as a pre-heater to a 114-L conventional electric water heater. Measurements and simulations indicate that fogging of the glass cover plates has reduced the transmissivity by around 63% over the 22 years.
© 2006 Published by Elsevier Ltd.

Keywords: Calibration; Simulation; Solar Collectors; Water Heating

1. Introduction

This study concerns the author's residence, which housed a family of five from 1982 to 1985, three people from 1985 to 1998 and two people from 1998 to 2005. The home had two storage-tank type water heaters serving two sections of the house. Both tanks contained two electric resistance 4500-W heating elements. One tank, 197 L (52 gal.), served the laundry area and two bathrooms. The second tank, 114 L (30 gal.), served the master bathroom and kitchen (with dishwasher). The solar system was originally installed to serve only the larger tank but was connected to both tanks 3 years later. Though the total daily hot water consumption for five people was around 379 L (100 gal.) per day, only 325 L (86 gal.) were used through the tank being served by solar and 54 L (14 gal.) by non-solar.

On 12 June 1982, the Sun-Pride solar system, manufactured by Revere Solar Products, was purchased for US$1160 and installed. No state sales tax was charged due to state law exempting energy devices. The closed-loop system included check valves, a by-pass tempering valve, pressure gauge and relief valve, pump, differential thermostat controller, shut off valves, air expansion tank, air vents, two $1.6\,m^2$ ($17.2\,ft^2$) collectors, and a 303-liter (80-gal.) storage tank with a heat exchanger near the bottom of the tank. The system is depicted in the schematic diagram in Fig. 1. The collector heat transfer fluid is a 50:50 mix of ethylene glycol and water.

Using a 1-m^2 ($10\,ft^2$) of collector per person rule-of-thumb, a third collector panel was purchased and installed along with the other two, resulting in a total collector area of $5\,m^2$ ($53.7\,ft^2$), or about $1\,m^2$ ($10.7\,ft^2$) per person. The solar tank provided about $60\,L/m^2$ ($1.49\,gal./ft^2$) storage/collector ratio. The final collector array is shown in Fig. 2.

The three collectors are patterned after the general collector design shown in Figs. 3 and 4. They are the flat-plate type with a double-glazed cover plate and a flat black absorber plate. The transfer fluid pattern is parallel flow from a bottom header to a top header with fluid exiting at the opposite upper corner from which it enters at the bottom.

The roof is oriented toward true South and has a pitch of $36°$, which is about $6°$ higher than the site latitude of $30°$N. This was considered to be ideal, so no further added tilt was necessary. There are no trees or other objects shading the collector panels. After all expenses were accounted for, the total cost of the system was US$1500. A 40% income tax rebate made the effective cost just $900, labor excluded,

E-mail address: larry@archone.tamu.edu.

Nomenclature

C temperature, Celsius

C_p mass specific heat, 4184 J/kg K (1 Btu/lb °F) for water

D_i inside diameter of aluminum tube, $= 0.016$ m (5/8 inch or 0.052 ft.)

Eff   solar collector efficiency (dimensionless)

F temperature, Fahrenheit

F_R Collector heat removal factor (dimensionless)

F' U_0/U_L = collector efficiency factor, the ratio of heat conductance factors for "fluid to ambient air" to "absorber to ambient air." The F' factor is mostly dependent on the absorber fin geometry and material, but it is not a strong function of plate temperature. For the collector plates in this study, the values for single plate vs. double plate covers were 0.94 and 0.97, respectively. These are based on values from page 145 in Duffie and Beckman [1] for aluminum absorber plates with 15 mm tube spacing

$h_{f,i}$ forced fluid heat transfer coefficient inside the tubes, $= 1500$ W/m^2 K (264.2 Btu/ft^2 °F h)

I_{DN} incident direct normal insolation (W/m^2)

I_{df} incident diffuse insolation (W/m^2) on tilt

I_T insolation on collector tilt $= I_{DN} \cos(\Theta_T) + I_{df}$

K   temperature, Kelvin

L total length of tube per collector area,- 6.67 m per m^2 (2.05 ft/ft^2), for a tube spacing of 0.15 m (6 inch)

Q_T solar radiation transmitted through the collector cover plates (W/m^2)

Q_u useful energy out of collector (W/m^2)

$\check{R}$ mass flow rate, $= 0.02$ kg/m^2 s (14.7 lb/ft^2 h)

t_a temperature of outside air (°C)

$t_{f,i}$ temperature of heat transfer fluid at collector inlet (°C)

$t_{f,m}$ mean fluid temperature (°C) in collector

τ transmissivity of cover plate.

Θ_T solar angle of incidence to collector panel

Trans (Θ_T) transmittance parameter at angle, Θ_T

U_B heat transfer coefficient for collector bottom, typically about 0.3–0.45 W/(m^2 K)

U_C heat transfer coefficient for cover plate, typically around 7 W/(m^2 K) for single plate and 3.7 W/(m^2 K) for double cover plates.

U_L overall heat loss coefficient (W/m^2 K)

U_p heat transfer coefficient between the plate and the fluid, equal to: $h_{f,i}$ (π) D_i L, $= 503$ W/m^2 K (88.5 Btu/ft^2 °F h)

x collector fluid parameter, $(t_{f,i}-t_a)/I_T$

or $180/m^2$ ($16.76/ft^2$). Using typical-year weather data, a software model (described later) was run to predict a solar heating contribution of around 80% and a simple payback on the investment of about 2.9 years.

In order to see if the computer simulation prediction was valid, electric kWh consumption records were made for 1 year prior to the installation of the solar system and for the year following the installation. The heating element at the top of the hot water heater was left activated at all times, but only turned on when there was not enough solar energy to preheat the water. In the first summer of operation, the electric element never turned on and showed consumption only after mid-October. After one year of operation, the measured electric use was 790 kWh compared to the prior year of 5011 kWh when no solar system was installed. The solar system was therefore giving slightly better performance than predicted, yielding about 84% of the annual needs and saving $312.34 a year. Since the total investment was $900, the payback is computed to be 2.88 years, approximately what the software had predicted. No attempt was made to correct for possible weather differences in the 2 years that were evaluated; however, when the calibrated simulation was performed, identical weather data were used for both years.

In 1985, the smaller "non-solar" water heater was removed, and the plumbing was rerouted so the solar system would serve all hot water use in the house through the 197-L tank. In 2004, this tank failed, was discarded, and the smaller water heater was installed in its place. Since this heater is much smaller than the previous one, both of the 4500-W heating elements were left activated.

For the 1982–2005 period, an estimate was made of the total savings in water heating energy. First, the base consumption was based on the consumption rate in 1981 with five persons present. This established a "daily-use-per-person" rate that was applied over the 22 years, during which three of the occupants left the household. Once the yearly consumption was determined, a cost savings estimate was calculated from known electric rates that increased only modestly from $0.074/kWh in 1982 to $0.08/kWh in 2005. The actual costs were determined precisely from the measured kWh consumption. The solar system netted an electric savings of about 44,647 kWh, for a cost savings of around US$3440. The annual savings in heating kWh are shown in the graph in Fig. 5. The graph clearly illustrates that the savings in 1982 were on the order of 80%, and the savings in 2004 have degraded to around 50%. The area between the two curves represents the aggregate savings of 44,647 kWh over the 22 years.

2. Procedures

During 1 year prior to the collector installation plus the first 2 years of operation, the kWh use was measured by use of a system-on timer. This enabled the calculation of kWh energy savings from the solar system. In the 22nd year, the

water temperatures were measured by time-dependent portable data loggers; thus, both water temperatures and system on-time usage could be analyzed. In the software simulations, hourly weather records were used to determine

Fig. 1. The Revere Sun-Pride system.

the incident solar radiation values and the ambient dry-bulb temperatures. By adjusting the collector cover plate transmission factor, the simulated annual water heating energy could be calibrated against the measured kWh consumption. Once the simulated energy consumption matched the measured results, monthly, daily and hourly values were also checked for agreement. Graph plots were then made of hourly measured and predicted tank temperatures for several week-long periods. This permitted the inspection of aggregate energy savings as well as time-dependent performance characteristics.

3. The solar simulation model

A FORTRAN program was written by the author, based on flat-plate solar collection methodology developed by Duffie and Beckman [1]. The program was designed to use either "typical" simulated weather [2,3] or recorded weather records. In 1982, the program was run using typical weather data and a collector efficiency equation published by the collector manufacturer. In 2005, locally recorded weather data were used, because the objective was to calibrate between measured performance and the simulated performance by adjusting the solar collector efficiency parameters.

Though the model can accommodate a variety of collector types, it is intended mostly to handle the category of flat-plate water-cooled collectors with tank storage. Sun angles and direct normal and diffuse insolation are derived on an hourly basis within the model, so concentrating and tracking collector systems may also be modeled with little extra effort [3].

The solar collection model computes the thermal energy output from the collector, after which the net useful energy is computed by doing a thermal balance on the storage tank. This is done by adding the collector heat minus the
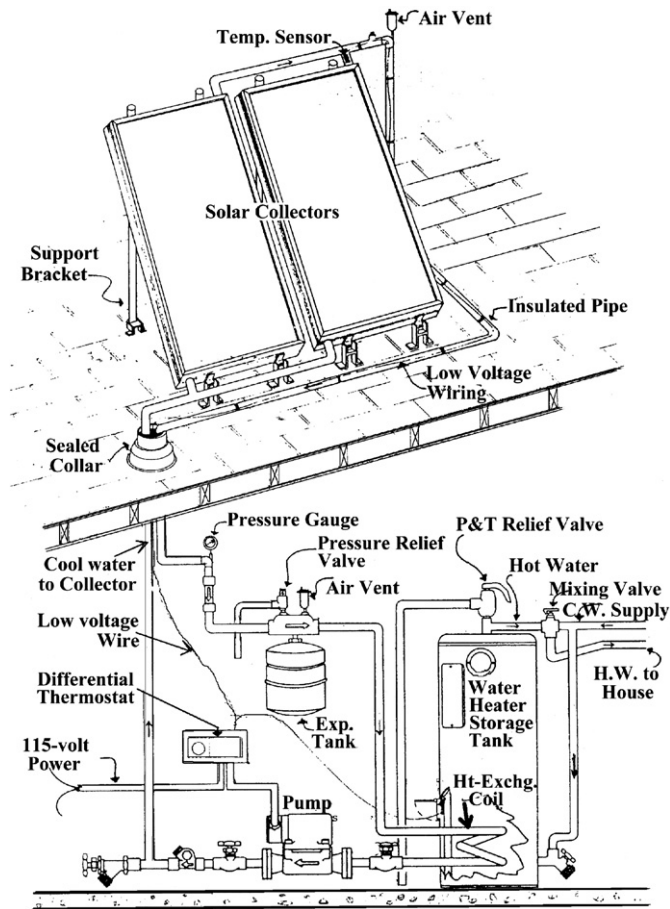

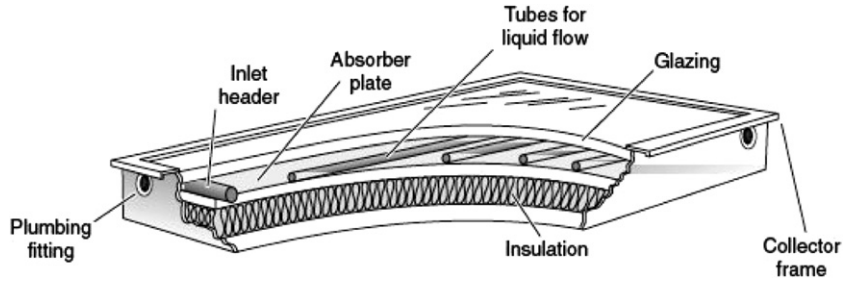Fig. 2. Exterior view of collector panel arrangement.

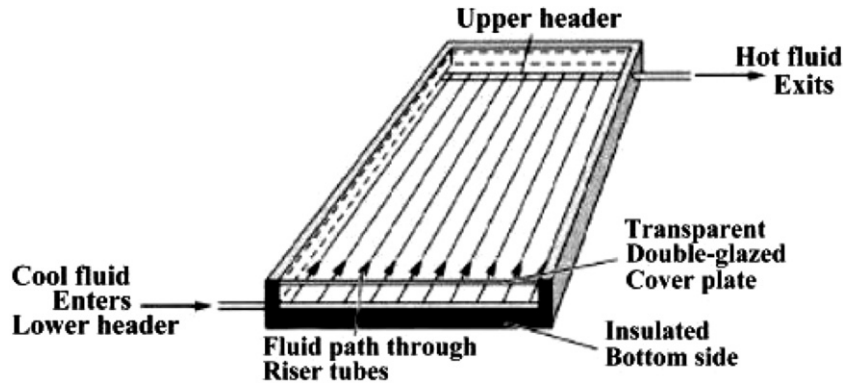Fig. 3. Cut-away section of the flat-plate collector design.

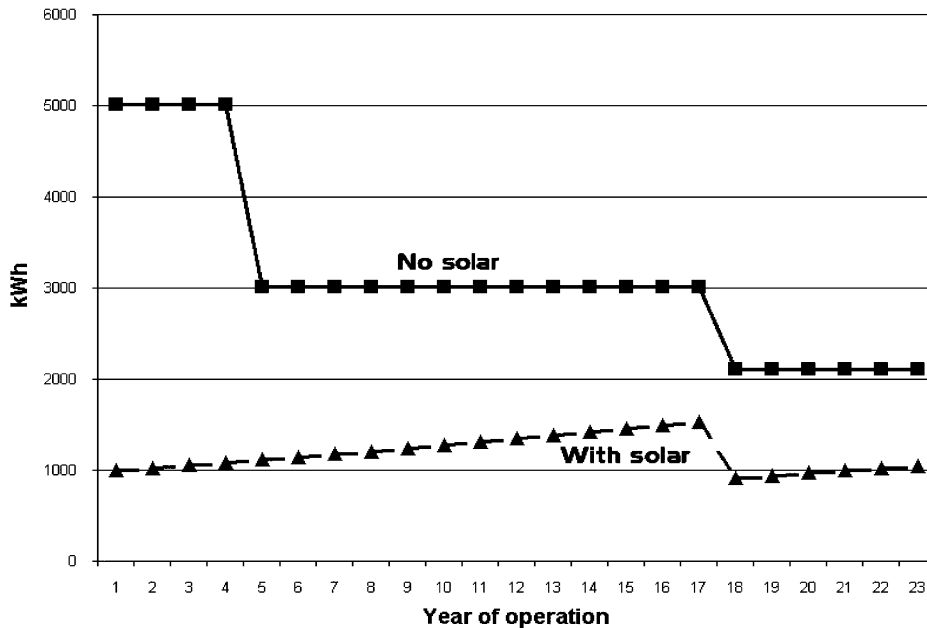Fig. 4. Fluid flow pattern in collector plates.

Fig. 5. Annual kWh energy savings by solar heating system.

building's hot water demand and tank losses. The tank water temperature is never permitted to exceed boiling, 100 °C (212 °F).

The collector's useful energy output is modeled using the Duffie–Beckman equation

$$Q_u = F_R[Q_T - U_L(t_{f,i} - t_a)]. \qquad (1)$$

Since F_R and U_L are themselves dependent on Q_u, the precise establishment of Q_u is an iterative process. The program was originally devised to iterate a series of equations to converge on an acceptably low error in Q_u, but repeated runs with the program revealed that a substitute one-pass series of computations would result in an acceptably accurate solution. This technique has

resulted in a very useful procedure for flat-plate collector output computations [4], the steps of which are delineated below

Step 1: Given I_{DN}, I_{df}, and sun angles, compute Q_T.

$$Q_T = \tau(I_{DN}\cos(\theta_T)\text{Trans}(\theta_T) + I_{df}). \tag{2}$$

Step 2: Set $t_{f,i}$ equal to the storage tank temperature.

Step 3: Set a temporary value of U_L at $4.0\,\text{W/m}^2\,\text{K}$, (or $0.7\,\text{Btu/ft}^2\,\text{F h.}$)

Step 4: Set a temporary value of F_R at 0.9.

Step 5: Compute a temporary value of Q_u, by Eq. (1).

Step 6: Compute mean fluid temperature based on a specified fluid mass flow rate

$$t_{f,m} = t_{f,i} + Q_u/(2\check{R}C_p). \tag{3}$$

Step 7: Compute mean plate temperature

$$t_{p,m} = t_{f,m} + Q_u/U_p. \tag{4}$$

Step 8: Compute the cover plate heat transmission coefficient (U_C). This is a function of number of glass cover plates, emissivity of absorber plate, wind speed, $t_{p,m}$ and t_a. For empirical equation, see [1, pp. 132–135].

Step 9: Compute the overall heat loss coefficient:

$$U_L = U_C + U_B. \tag{5}$$

Step 10: Compute the collector heat removal factor

$$F_R = (\check{R}Cp/U_L)[1 - \exp(-F'U_L/\check{R}Cp)]. \tag{6}$$

Refinements in the value of Q_u can be obtained by iterating the above sequence beginning at Step 5 and going through Step 10; however, it was determined after several computer runs that a one-pass process may result in sufficiently accurate results.

Step 11: Compute final value of Q_u, by using Eq. (1).

The above steps are utilized by the computer program when a certified and published efficiency graph is not available for the collector. If an efficiency plot is available, then it can be used to compute Q_u in lieu of iterating the 11 steps shown above. The form of the efficiency equation is

$$\text{Eff} = A - Bx - Cx^2, \tag{7}$$

where Eff is the collector efficiency; x the fluid parameter A, B, C = regression coefficients.

For the Sun-Pride system, the published equation (in inch–pound units) was

$$\text{Eff} = 0.77 - 0.549x - 0.3x^2. \tag{8}$$

Step 12: Compute storage tank losses: The hot water demand is determined from an hourly use pattern, thus drawing in new supply water and lowering the tank's temperature. The tank's stand-by losses are determined by multiplying the tank's surface area by the shell's U-factor and the temperature difference to the room's ambient temperature. The tank's surface area is $2.35\,\text{m}^2$ ($25.33\,\text{ft}^2$) and the U-factor is estimated to be $0.57\,\text{W/(m}^2\,\text{K)}$, or $0.1\,\text{Btu/(h ft}^2\,\text{F.})$

A plot of the performance curve is shown in Fig. 6. This is a typical shape of an efficiency plot, showing that as a collector's temperature is increased, the efficiency decreases because of increased heat losses to the ambient air. The intercept on the y-axis (0.77) is essentially the collector's efficiency when the collector's temperature is equal to the outside air temperature; i.e., no heat losses from the collector. This intercept is, therefore, a close indicator of the cover plate transmissivity. The fluid parameter on the horizontal axis is actually the temperature difference between the incoming water and the outdoor ambient air divided by the incident solar radiation flux.
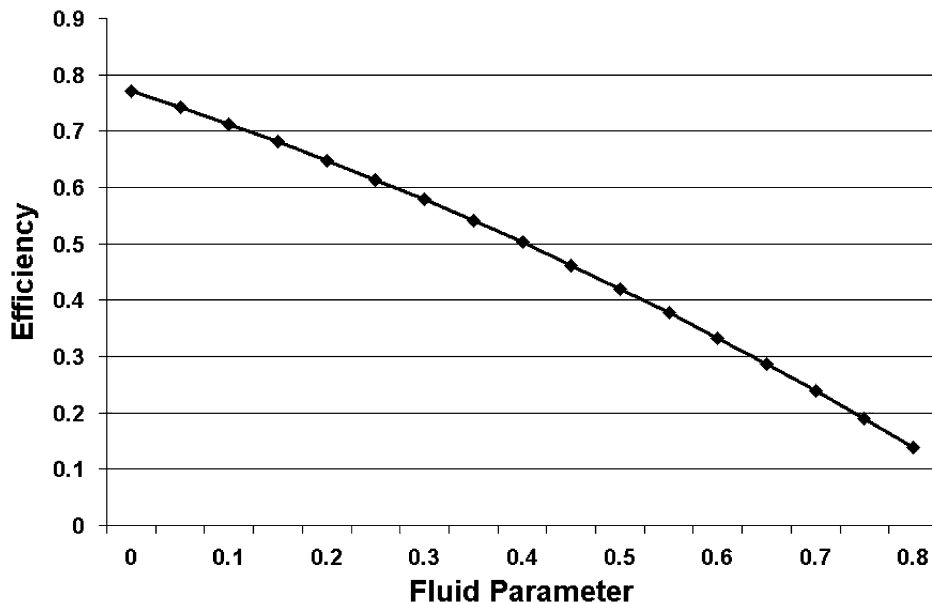

Fig. 6. Original Sun-Pride efficiency curve.

3. Measurement results

Detailed temperature measurements were made through-out 2004 at 3-min intervals by portable data loggers. Recorded data included the temperature of the fluid returning from the collector, water temperature near the top of the storage tank, and the room temperature where the storage tank and water heater were located. This is a small room with an outside door that has 0.28 m^2 (3.03 ft^2) of glass facing due south. This aperture allowed for natural solar heating of the space surrounding the solar storage and water heater tanks, typically keeping the room around 27–29 C (80–85 °F) throughout the day and night and thus minimizing the standby heat losses from the tanks. A typical plot of temperature data from December 2004 are shown in Fig. 7.

This plot shows temperatures for outdoor, tank room, water in top of storage tank, and water returning from the collector. In addition, it shows hourly horizontal global insolation for a 2-day period. (Inch–pound units, °F and Btuh/ft^2, were used for this graph so the values for both temperature and insolation could be scaled easily on the same axis.) From the graph, it can be seen that the room temperature is typically 20–25 °F (11–14 °C) warmer than the outdoor temperature. This is due to the solar gain through the south-facing window in the door, as the room is neither heated nor cooled by the house HVAC system. In addition to temperature data, the electricity consumption was monitored continuously through the use of timers attached to both heating elements in the water heater. The kWh consumption was then derived by multiplying the timer hours by 4500 W (the actual rating of each element.)

Hot water usage was measured over a period of one month to determine the typical consumption pattern for the two residents of the house in 2004. The consumption rate was 136 l (36 gal.) per day, or 68 l (18 gal.) per person per day. The temperature rise was typically from 20 °C (68 °F) incoming temperature to about 54 °C (129 °F) outgoing temperature. This resulted in a temperature of about 51 °C (124 °F) at the faucet.

Using the measured base data, an annual consumption was calculated to be 49,871 l (13,176 gal.). The annual heating of this water was computed to be 2414 kWh, or about US$193, if no solar system were present. The mea-sured consumption, with solar present, was 1060 kWh, or about US$84.80. This means that the annual solar contribution is 56% as compared to the 84% solar contribution during the system's first year of operation 22 years earlier.

4. Simulation results

The simulation model was run for the year of 2004 using actual outdoor temperature and solar radiation data recorded at a local site. Using repeated computer runs, it was possible to match the annual 56% solar contribution by varying the collector's efficiency by successively low-ering the A-coefficient in the efficiency equation, which approximates the actual transmissivity of the cover plate. An annual energy match was made when the A-coefficient was 0.28. This is a radical reduction from the original 0.77 value when the collector was first installed. This can be supported somewhat by visual confirmation that the cover plates are no longer transparent. Instead, they have been
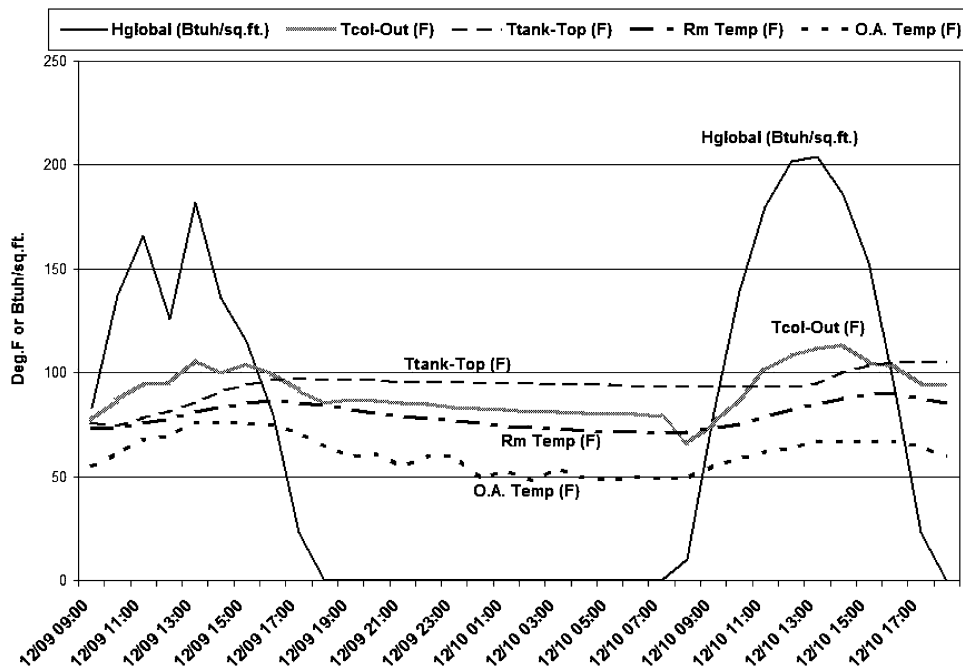

Fig. 7. Typical plots of measured data, 9–10 December 2004.

severely whitened by a chalk-like substance on their interior. At this point, no effort has been made to remove the plates, clean and re-seal them. The new efficiency curve is therefore

$$\text{Eff} = 0.28 - 0.549x - 0.3x^2. \qquad (9)$$

To show the magnitude of this degradation from the original performance, a plot was made (Fig. 8).

In order to confirm that the new efficiency equation would satisfactorily predict hourly energy collection performance, several plots were made of selected periods of the year, specifically, early August, mid-September, and mid-December. These plots are 6–9 days in length and show hourly results for calculated temperatures in the storage tank and recorded temperatures for tank (top), collector out, and outdoor ambient. Hourly global insolation values are shown as well. These plots are shown in Figs. (9–11). Once again, inch–pound units are used for scaling reasons.

The previous three figures show hourly values of measured outdoor dry-bulb temperatures, horizontal global insolation, water temperature leaving the collector, and temperature in the storage tank. Included is also the simulated tank temperature, for comparison to the
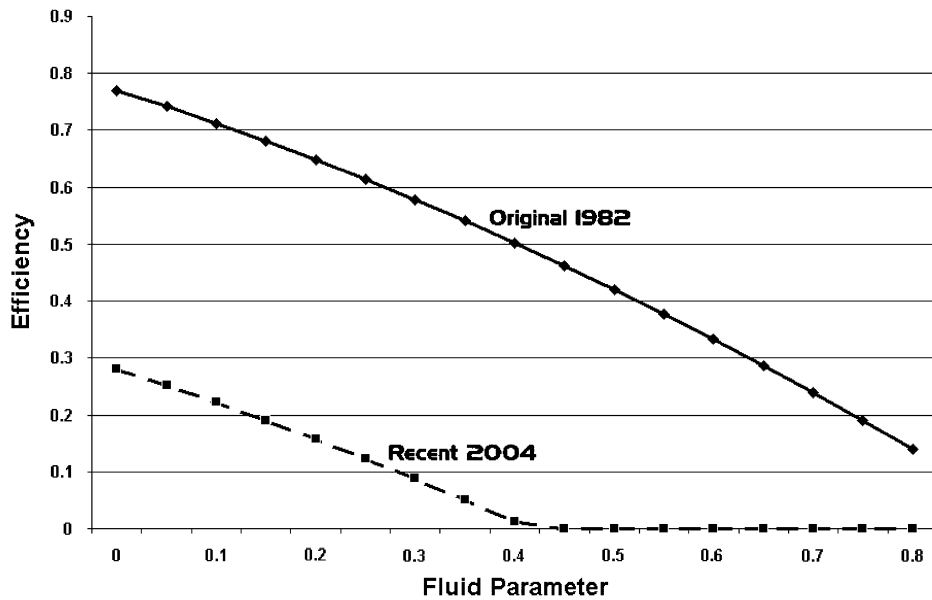

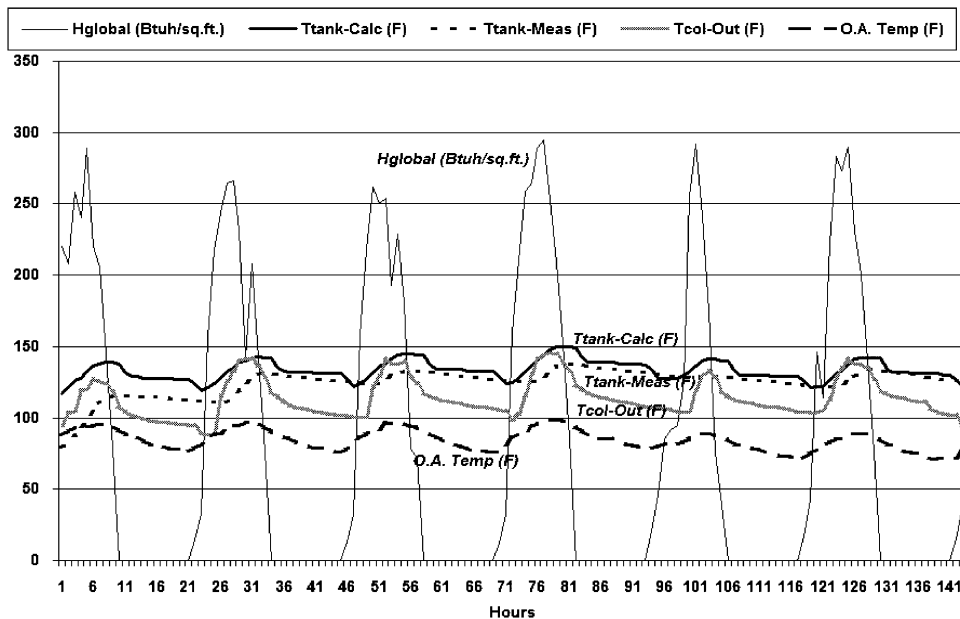Fig. 8. Efficiency curves—year 1982 vs. 2004.

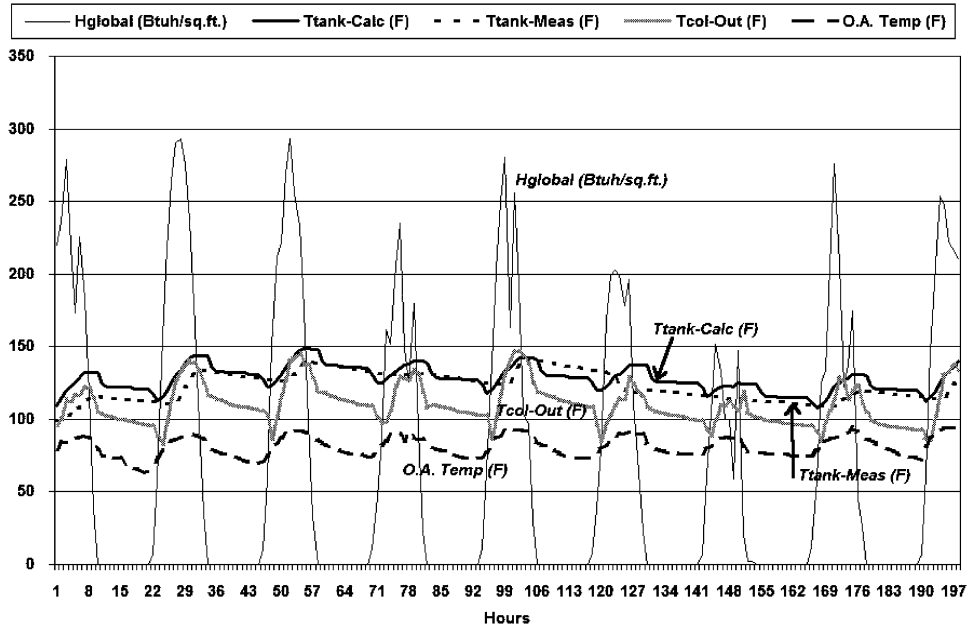Fig. 9. Calculated and measured temperatures (2–8 August 2004).

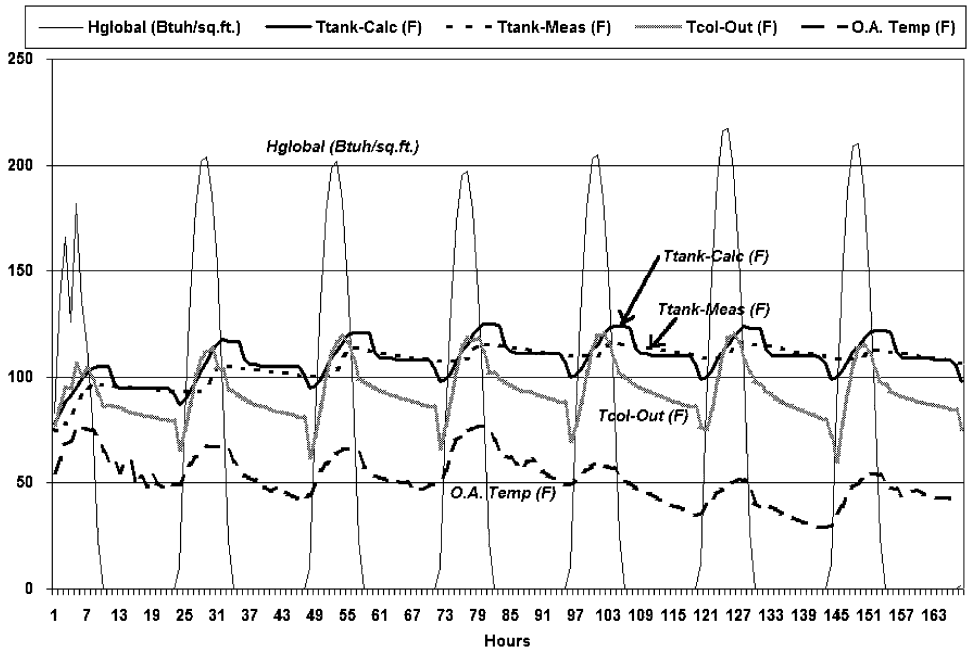Fig. 10. Calculated and measured temperatures (8–16 September 2004).

Fig. 11. Calculated and measured temperatures (9–16 December 2004).

measured tank temperature. Since the simulated tank temperature is a "mixed" temperature, it should not be compared directly to the measured value of "top of tank" temperature. These do have a close relationship, but because of tank stratification, the "top of tank" temperatures will tend to reach a higher value than the mixed tank temperature. Another factor in trying to make exact comparisons of hourly temperatures is that the real hot water use pattern will not follow the assumed use pattern that is in the computer program. The average

daily use in the simulation is the same as the actual average daily use, but the day-to-day use amounts were not measured. This will cause the comparison to be high on some days and low on others, as can be seen in the plots in Figs. (9–11).

In addition to comparing hourly temperatures and annual energy consumption, it is of interest to observe some of the monthly statistics of weather, solar and water heating energy supplied by solar. To observe this, a plot was made of the monthly percent load supplied by solar
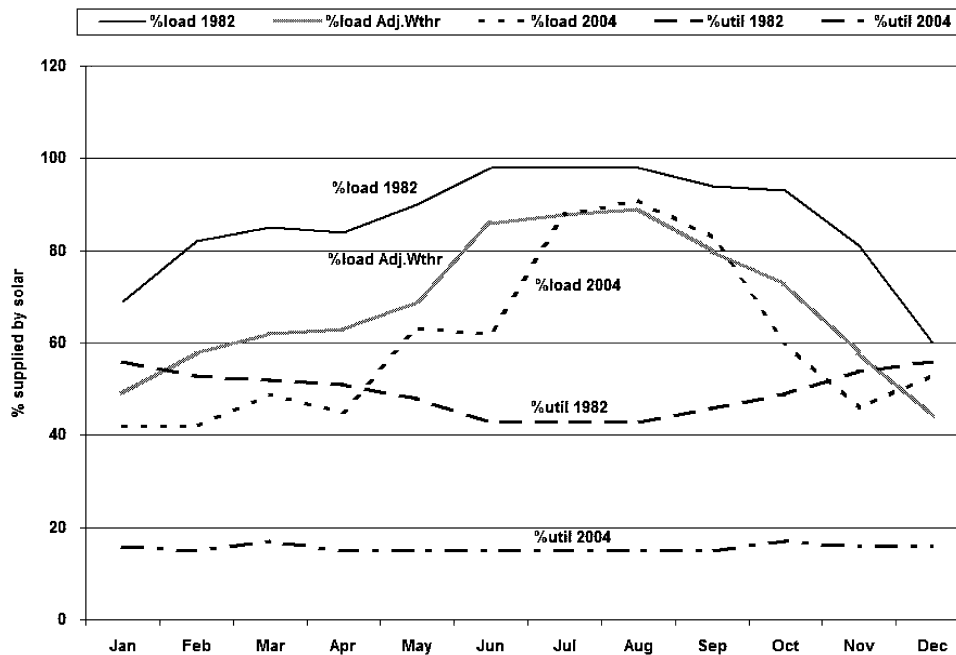
Fig. 12. Monthly percentage load supplied by solar and collector energy utilization efficiency.

energy in both the original 1982 scenario and the one existing in 2004. The plot also includes the monthly percentage solar energy utilization efficiency by the collector (see Fig. 12).

In Fig. 12, the percent utilization efficiency (% util 1982) is quite different than the percent of load supplied by solar energy (% load 1982), and these are both different than the collector's output efficiency. The percent of load supplied by solar is the total solar energy delivered divided by the total water heating demand by the household. The utilization efficiency is the amount of collected solar energy used divided by the total energy incident on the collector. The latter is influenced not only by the collector's efficiency (ability to convert incident energy into usable heat), but also by the hot water demand by the household. If a collector is large and the demand is small, then the utilization efficiency will be small. Such is the case for this experiment. When the collector was initially installed the household consisted of 5 users and the utilization efficiency was high, around 50–90%. In 2004, there were only two users, so the demand was smaller and the utilization efficiency reduced to 15–17%. The smaller demand coupled with the fact that the collector's performance has been degraded over the years has resulted in low utilization efficiency. This became quite evident in the plot shown in Fig. 12.

Fig. 12 also shows that the solar system's monthly contribution to the water-heating load varied between 60% and 98% in 1982 and from 41% to 91% in 2004. Had the collector performance not degraded, one would expect the heating load contribution to actually increase on a percentage basis, since the hot water demand had been reduced from 5 to 2 people over during this period.

However, the collector performance was severely degraded, so the energy contribution was lessened. It is noteworthy to point out a weather-related factor—the annual solar radiation in 2004 was just 86% of that used in the calculations for 1982. To get a more accurate picture of the collector's performance in 2004, the same weather data used in 1982 was then applied to the year 2004. The results of that simulation are also shown in Fig. 12, and are labeled as "% load Adj.Wthr." This curve shows a somewhat better performance in 8 months, one equal, and 3 less (August, September and December.) The low and high values are similar to before (about 42–90%), but when summed on an annual basis, the annual water heating supplied by solar increased to 65% from the previous value of 56%.

It was of interest to see if there are differences in the system performance predicted by the two simulation models utilized. The comparison was made for the current system for the year 2004 when using the Duffie–Beckman method with collector properties vs. the manufacturer's efficiency curve method. For the Duffie–Beckman model, Eqs. (1)–(6) were used along with the 11 computational steps outlined earlier, with the cover plate transmissivity (τ) set at 0.37. This yields an overall collector efficiency of around 0.28 on the Y-intercept (F_R) when the collector is in a neutral state with the surrounding ambient air. For the model that used the manufacturer's efficiency curve, Eq. (9) was used. After the simulations were run with the two models, plots of the monthly solar contributions to the heating loads were made as shown in Fig. 13. As can be seen from the graph, the two methods produce indiscernible differences in March, April and June–November. The Duffie–Beckman model predicts slightly

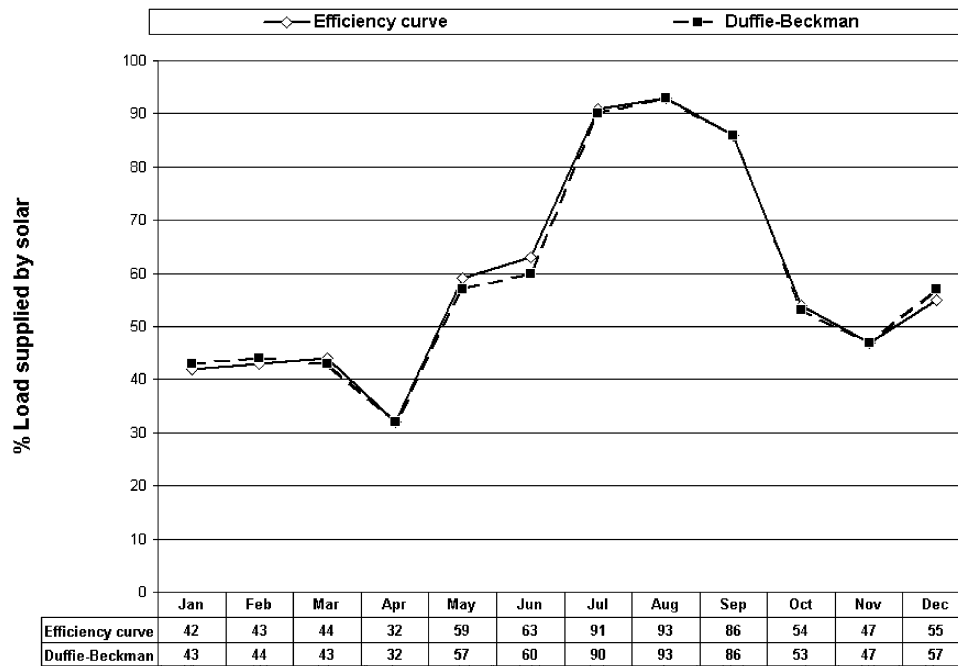|	Jan	Feb	Mar	Apr	May	Jun	Jul	Aug	Sep	Oct	Nov	Dec
Efficiency curve	42	43	44	32	59	63	91	93	86	54	47	55
Duffie-Beckman	43	44	43	32	57	60	90	93	86	53	47	57

Fig. 13. Comparison of system performance between the Duffie–Beckman method and the efficiency curve method.

less contribution in the months of May and June and slightly greater contribution in December, January and February (the cloudier months).

5. Conclusions

In general, the simulated hourly temperatures do align adequately with the measured values, at least enough to not have serious doubts about anomalies in the simulation process. Furthermore, the annual energy results show very close correspondence between measured and simulated values.

The study made it quite obvious that the collector performance has deteriorated markedly over its 22-year life. The first assumption made in this study was that this deterioration was due to clouding of the collector plates. By lowering the transmissivity only, and leaving all other factors in tact, the simulations seem to closely corroborate the measured results of annual energy predictions. Furthermore, the model seems to have fair success in tracking the hourly temperature data.

There are other factors that could contribute to lowering of collector performance. Since the collector panels are arranged in parallel, it is not known whether there may be dirt stoppage in one or more of the pipes serving the three collector panels. If that were the case, it could also explain some of the degradation in performance, but from a simulation perspective, the lowering of cover plate transmissivity seems to also provide an adequate explanation of the degraded performance.

The next step in this study will be to remove and clean the cover plates and measure the performance for another year. It will be of interest to see if much of the losses can be recovered by restoring some of the cover plates' original transparency.

References

[1] Duffie JA, Beckman WA. Solar energy thermal processes. New York: Wiley; 1974.
[2] Degelman L. Simulation and uncertainty: weather predictions. In: Malkawi, Augenbroe, editors. Advanced building simulation. New York and London: Spon Press; 2004. p. 60–86 (Chapter 3).
[3] Degelman LO, A statistically-based hourly weather data generator for driving energy simulation and equipment design software for buildings. In: Proceedings of the building simulation '91, International Building Performance Simulation Association (IBPSA), Nice, Sophia-Antipolis, France, 20–22 August 1991. p 592–9.
[4] Degelman LO, Computer optimization of solar collector area based on life-cycle costing. In: Proceedings of the 1977 annual meeting of the International Solar Energy Society (ISES), Orlando, FL, 16–19 June 1977, vol. 1, p. 8–15.
[5] Degelman LO. Calibrated simulation of the degradation of a solar hot water system performance over a 22-year period of operation. In: Proceedings of the building simulation 2005, 9th International Building Performance Simulation Associationn (IBPSA) Conference, Montreal, Que., 15–18 August, 2005. p. 247–54.